PHYSICAL REVIEW A VOLUME 34, NUMBER 1 JULY 1986

Flow patterns and nonlinear behavior of traveling waves in a convective binary fluid

Elisha Moses and Victor Steinberg
Department of Nuclear Physics, Weizmann Institute of Science, Rehovot 76100, Israel
(Received 28 March 1986)

Flow visualization, heat-transport measurements, and the light-intensity profile as a function of time have been used to study nonlinear propagating waves in ethanol-water mixtures heated from below. The experimental results reveal the main features of the traveling waves predicted by recent theory.

Traveling waves in a confined volume of binary fluid heated from below are a feature not quite expected by theory.[1] Previous discussions of the oscillatory instability in double diffusive systems dealt with the simpler case of standing waves[1,2] Not surprising is the fact that traveling waves have been observed[2(b)] in a binary mixture, a system that has revealed a remarkable variety of dynamic behavior due to the interaction between heat diffusion and mass diffusion. Linear stability analysis of a binary mixture near the convection threshold predicts that the convective state will be oscillatory or stationary, depending on the value of the separation ratio ψ, a measure of the coupling between temperature and concentration variations.[3] For sufficiently negative values of ψ the theory predicts a transition to a periodic state.[3] For larger values of ψ the bifurcation at critical Rayleigh number $R_{cs}(\psi)$ leads to steady convection.[3] These two instability branches intersect in the R-ψ plane at the codimension-two (CT) point when $\psi=\psi_{CT}<0$.[1,3]

Recently a theoretical treatment of double diffusive systems has been proposed which views traveling and standing waves as different manifestations of an underlying O(2) symmetry of the infinite system. In this framework, traveling waves in binary mixtures are preferred to standing waves near onset for a wide range of ψ. Features that might also be expected to be robust and observable in experiments with realistic boundary conditions are the following: (i) The effective-heat-flow measurements should not show oscillations, except for a small amplitude modulation at frequency $2f$, due to the presence of side walls. (ii) The branch of traveling waves should terminate in a steady-state bifurcation and the frequency of the waves should vanish linearly while approaching a heteroclinic orbit. (iii) The transition to steady overturning convection should be hysteretic.

Since for an infinite system the stationary and traveling wave states are indistinguishable in heat-transfer measurements, previous understanding of the oscillatory instability through heat-flow measurements gives information that is highly dependent on the interaction between the waves and the lateral boundaries. In order to give a quantitative picture of the properties of nonlinear propagating waves, direct optical measuring techniques must be applied. To get this quantitative information, we have conducted an investigation of the properties of traveling waves close to the CT point, where finite-amplitude effects are small. Results for nonlinear behavior in the close vicinity of the CT point will be published elsewhere.

We present here observations of flow patterns, simultaneous high-resolution heat-transfer measurements, and light-intensity measurements as a function of time and locations in the flow ("line scan" and "contour") in a room-temperature experiment, using ethanol-water mixtures of negative ψ in the vicinity of the CT point. The value of ψ was varied by changing the mean concentration of the mixture and the mean operating temperature of the sample. Our detailed study reveals the following main features of nonlinear traveling waves. (i) The traveling waves move across the cell with the constant velocity $V=2df$ (d is the height of the cell); a new roll continuously appears on one side of the cell and another one disappears on the opposite side of the cell without pinning. (ii) The velocity of the propagation (or frequency) decreases monotonically to zero as the amplitude increases. The branch of traveling waves terminates in a steady-state bifurcation and the frequency of the waves vanishes linearly with the distance from a heteroclinic orbit, as predicted by theory.[4] (iii) The transition to steady convection is backward and hysteretic, as predicted by theory.[4] (iv) For the cell with the larger aspect ratio and even number of rolls, heat-flow measurements show oscillations with very small or zero amplitude. Nevertheless, for a smaller aspect ratio and odd number of rolls the oscillations of the effective heat transport are big, with frequency f and with a modulation of frequency $2f$. The largest amplitude of the modulation is as large as 2 mK at ΔT_c on the order of 2 K, i.e., the maximum modulation is 0.1%. (v) The range of R over which the traveling waves are observed decreases toward the CT point. (vi) For more negative values of ψ, disordered flow patterns and chaotic time behavior in "line-scan" measurements are observed close to the heteroclinic orbit.

The experiments were done on ethanol-water mixtures with ethanol weight concentration in the range 25% to 28% and in the temperature range between 22 and 35 °C. This fluid mixture was chosen because it gives the opportunity to tune ψ over a wide range by changing the mean temperature and concentration of the sample. The crucial factor in our choice of fluid was that the thermodynamic and transport properties of the mixtures as function of T and c are known very well, aside from the thermodiffusion ratio k_T. The latter changes sign somewhere between 28 and 30 wt.% of ethanol at 25 °C.[5] Since the experimental data on the temperature and concentration dependence of k_T are very poor, the uncertainty in the location of our measurements on the R-ψ plane is fairly large, particular-

ly close to the CT point. Therefore, we used the ψ dependence of the critical Rayleigh number R_{co} on the oscillatory branch obtained from linear stability analysis to estimate ψ for our samples.[3] From these estimates our measurements cover the range $-0.12 \lesssim \psi \lesssim -0.02$.

Our experimental apparatus is an improved version of the one described previously.[6] The temperature stability of the bottom plate was better than 0.1 mK during many hours with the noise on the level of 0.1 mK rms. Special care was taken to improve the shadowgraph technique of the flow-pattern visualization: We were able to resolve the patterns already at $\varepsilon = 10^{-3}$ [$\varepsilon = (\Delta T - \Delta T_c)/\Delta T_c$].

The convection cell is 2.96 mm high, 12.0 mm wide, and 36.0 mm long (the aspect ratio is 1:4:12; we used also another cell 3.98 mm high with aspect ratio 1:3:9). The bottom plate of the cell is made from copper, plated with Ni, and diamond machined in order to get a high-quality mirror surface. The top is sapphire, and the side walls are made of high-density polyethylene with a thermal diffusivity close to that of the fluid. The bottom plate is heated with a constant power. In order to study the oscillatory convection in detail, several types of measurements were performed simultaneously: high-resolution heat-flow measurements; flow-pattern visualization using a shadowgraph technique with computer-based enhancement and image processing; light-intensity measurements at several chosen locations in the cell as a function of time (line scan); and finally, light-intensity measurements on the line along the cell as a function of time (contour plot). Since the local temperature gradient in the fluid is proportional to the light intensity in a shadowgraph (at least, close to the convective threshold), we used the latter two techniques to observe local oscillations in the fluid and to study the propagation mechanism of the waves.

Figure 1 shows the dependence of the Nusselt number N (i.e., the ratio of the heat transport through the layer to that due to thermal conduction alone) versus temperature difference across a layer for 26 wt.% ethanol and a top-plate temperature of 28.185 °C. The jump in N observed for this sample is of order 6%. The hysteresis observed between the onset of the convection on heating and cessation on cooling is of the same order of magnitude (~50 mK, or 2%). Convection was originally stationary (we observed that on the line scan and on the contour plot) and evolved very slowly during several hours to being oscillatory. In a transient regime high-frequency oscillations were developed first with a frequency close to the neutral frequency predicted by linear stability analysis[3] (up to 10 mHz). However, on the stable oscillatory branch the observed neutral frequency for the sample was about 5 times less than that predicted by the theory. On cooling, the highest frequency observed was about 50% higher. Thus, the period of motion was considerably larger than, e.g., the vertical diffusion time $t_v = d^2/K$, which is 85 sec for this sample.[7]

The flow patterns observed near onset in the sample were very regular parallel rolls with wavelength $\lambda = 2d$ [Fig. 2(a)]. When one proceeds along the convective branch a disordered pattern appears near a heteroclinic orbit [Fig. 2(b)]. We discuss this observation later. On the stationary branch above the heteroclinic line the pattern

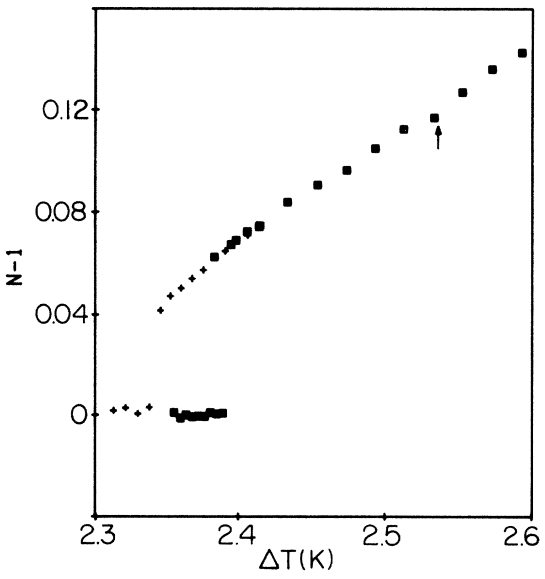

FIG. 1. Convective contribution $N-1$ to the Nusselt number N as a function of the temperature difference across the cell for 26 wt.% of ethanol and the temperature of the top plate is 28.185 °C. Approximate value of the separation ratio ψ is −0.1. Squares (crosses) are taken with increasing (decreasing) ΔT. The arrow shows the onset of stationary convection.

again becomes regular [Fig. 2(c)]. Figure 3 shows oscillations of light intensity at chosen locations in the cell (averaged along the height) for different ΔT. As one increases ΔT, one approaches the line of a heteroclinic orbit. Two phenomena were observed near the point of a heteroclinic orbit. First, the frequency oscillations decreased when ΔT increased. The lowest frequency we observed in the sample was 0.1 mHz, then the next small step in ΔT led the system to a steady flow. This transition is hysteretic.

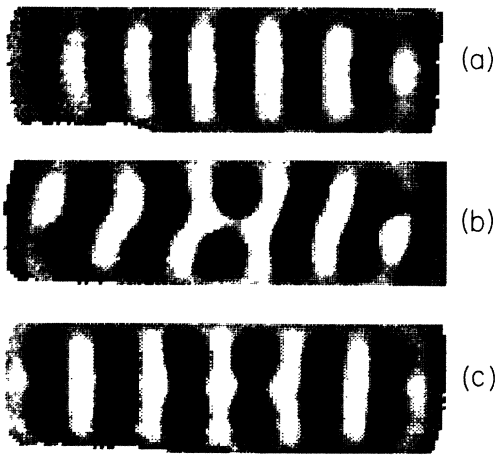

FIG. 2. Observed flow patterns in the cell with aspect ratio 1:4:12 for the sample 26 wt.% of ethanol at 28.185 °C. (a) Image of the flow patterns on the oscillatory convection branch; (b) image of "disordered" flow patterns on the oscillatory convection branch close to the point of the heteroclinic orbit; (c) image of the flow patterns on the stationary branch above the point of the heteroclinic orbit.

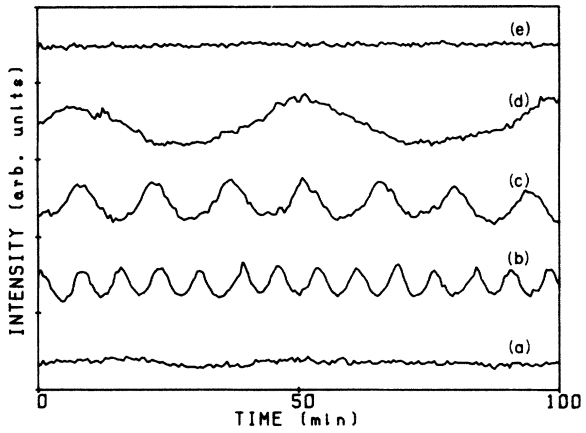

FIG. 3. The light intensity of a shadowgraph at the chosen location at the cell for the sample 26 wt.% of ethanol at 28.185 °C. (a) At $\Delta T = 2.385$ K on heating; (b) at $\Delta T = 2.3456$ K on cooling; (c) at $\Delta T = 2.4142$ K on heating; (d) at $\Delta T = 2.5337$ K on heating; (e) at $\Delta T = 2.5727$ K on heating.

Secondly, on the graph N vs ΔT it can be seen that a typical reduction in slope precedes the new bifurcation. We studied also the hysteretic behavior of finite-amplitude stationary convection on different samples. The hysteresis in frequency was observed along the oscillatory branch only if stationary convection had been reached on heating. The behaviors of both N and the frequency are reproducible on heating and cooling when one studies only the oscillatory branch. The dependence of the frequency (velocity) of the traveling waves on the distance from the point of a heteroclinic orbit is demonstrated in Fig. 4 for several samples. Linear behavior, predicted by the theory for traveling waves,[4] is clearly seen from the data.

Oscillations in N were also observed in these samples. They were not as regular as in the line scan and were at the main frequency f with modulation at $2f$ and of amplitude as large as about 1.5 mK at the lowest frequency. The fact that the observed time-dependent behavior is due to translation of the rolls with velocity $V = 2df$ was proven by mapping the light intensity along the line across the cell as a function of time (contour) (Fig. 5). It is clear from the "contour" that the waves propagate to the left with constant velocity V, and a new roll appears on the right-hand side of the cell and another roll disappears on the left-hand side without pinning.[8] As a consequence of the propagating waves in the finite-geometry cell which hydrodynamically transfer the mass, the question arises whether there are backflow effects. This backflow probably exists in the form of a long roll the size of the cell. The backflow should change the velocity distribution across the cell in the case of traveling waves compared with the case of stationary convection. This velocity redistribution would cause a redistribution in the field of the refraction index. If the backflow were located mostly near the top and the bottom of the cell, it would cause flattening of the light-intensity profile for the traveling waves. If, on the other hand, the backflow were located mostly near the side walls, the difference in length of the rolls in oscillatory versus stationary convection should be observed in the intensity profile along the rolls. We checked both possibilities and found that within our resolution no flattening appears, while the length decreases as propagation velocity increases up to an effect of 10%. Then the backflow velocity should be much larger than the propagation velocity of the waves. It would be interesting to measure this effect by using, for example, laser Doppler velocimetry technique. The backflow may change the picture considerably near threshold, since the existing model of the amplitude equation for propagating waves[4] has been derived for an infinite layer, without taking into account the backflow roll.

As a result of the wave propagation we observed a spatial inhomogeneous distribution of the refraction index in the conducting state (which corresponds to an inhomogeneous density distribution in the horizontal plane of the cell) after the convection ceased. This inhomogeneity increases the thermal conductivity λ_0 below threshold up to

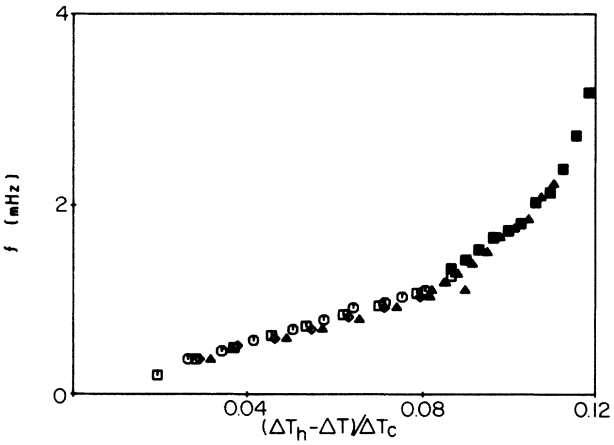

FIG. 4. The frequency of the oscillations f (or the velocity of the wave propagation) as a function of the distance from the point of the heteroclinic orbit for four samples: (a) triangles, 26 wt.%, 28.185 °C (solid triangles on cooling in hysteretic region); (b) squares, 25.5 wt.%, 29.15 °C (solid squares on cooling in hysteretic region); (c) diamonds, 25 wt.%, 29.6 °C; (d) circles, 26 wt.%, 30.2 °C.

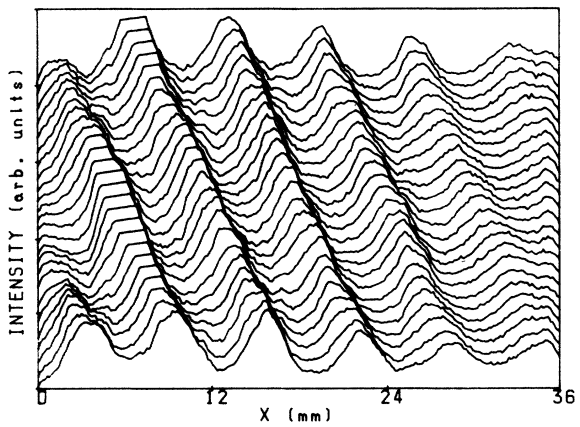

FIG. 5. The light intensity profile along the line in the cell as a function of time (contour plot) (time difference between successive profiles is 1.5 min).

1%, and then gradually disappears, but on a time scale of days. However, quenching from stationary convection to the conducting state returns the system to a homogeneous density distribution with λ_0 equal to its value before convection. An additional phenomenon that we persistently observed on the oscillatory branch was the appearance of disorder and irregularities in the patterns and noise in the oscillations on the line scan close to the heteroclinic orbit. It was observed in all samples with more negative ψ as a precursor of the bifurcation to a steady state [Fig. 2(b)]. It is worth mentioning that in these cases rolls were generated in one corner of the cell and continuously moved to the opposite corner as was observed previously in the experiment of Ref. 2(b).

As mentioned above, we estimated ψ for our samples using the ψ dependence of R_{co} from the linear stability analysis for the mixture with Lewis number $L=D/K \simeq 0.02$. Figure 6(a) shows the linear stability curve for our samples, together with the measured saddle-node and heteroclinic orbit curves. For larger ψ the smallest hysteresis was just 15 mK, i.e., on the order of 0.75%. At the same time, the smallest jump in N for this sample was 2.3% [Fig. 6(b)]. The closer to the CT point the narrower was the region of the oscillatory behavior on the finite amplitude convective branch; the smallest one was $\Delta T_h - \Delta T_c \simeq 40$ mK. Figure 6(c) shows also the neutral frequencies f_c observed for the different samples. For the region in ψ below -0.08 we observed higher values for f_c (or V_c), propagation was always to the left, and the pattern and the temporal behavior near the threshold was very regular. On the other hand, in the region in ψ above -0.08 were observed waves propagating to the right as well as to the left. The pattern and temporal behavior near threshold was very irregular for some runs and values of f_c were much lower and did not depend on ψ. Furthermore, we observed multistability of the system: Different patterns and different spatial and temporal behavior for the same set of the parameters (R,ψ) were found. Since this paper concentrates on general features of the nonlinear traveling waves, the latter phenomena will be the subject of a separate publication.

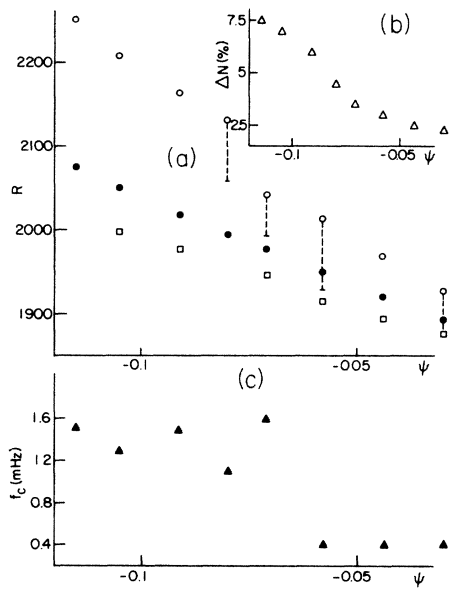

FIG. 6. (a) Stability diagram of ethanol-water mixture with $L=0.02$ heated from below. Solid circles correspond to the convection onset, and values of ψ were calculated using equation $R_{co}(\psi)=1800(1+L)(1+\psi)^{-1}$ [Ref. 3(c)]. Open circles are points of the heteroclinic orbit, and squares are the saddle node points. The broken lines show hysteresis regions of stationary convection for several samples. (b) Jump in the Nusselt number at the convection threshold (triangles). (c) Neutral frequency vs ψ (solid triangles).

We would like to thank H. Brand for helpful conversations. We are grateful to J. Fineberg for his contribution to the experiment. This work was supported by a U.S.-Israel Binational Science Foundation Grant, No. 8400256. One of us (V.S.) acknowledges the support of M. M. Bouckstein Career Development Fund.

[1]H. Brand and V. Steinberg, Phys. Lett. **93A**, 333 (1983); H. Brand, P. C. Hohenberg, and V. Steinberg, Phys. Rev. A **27**, 591 (1983); *ibid.* **30**, 2584 (1984); E. Knobloch and M. R. E. Proctor, J. Fluid Mech. **108**, 291 (1981); L. Da Costa, E. Knobloch, and N. O. Weiss, *ibid.* **109**, 25 (1981); D. Moore, J. Toomre, E. Knobloch, and N. O. Weiss, Nature **303**, 663 (1983); P. N. Coullet and E. A. Spiegel, SIAM J. Appl. Math. **43**, 776 (1983); for a recent review, see J. K. Platten and J. C. Legros, *Convection in Liquids* (Springer, New York, 1984), Chap. IX.

[2](a) I. Rehberg and G. Ahlers, Phys. Rev. Lett. **55**, 500 (1985); (b) R. W. Walden, P. Kolodner, A. Passner, and C. M. Surko, *ibid.* **55**, 496 (1985); (c) I. Rehberg and G. Ahlers, in *Multiparameter Bifurcation Theory in Contemporary Mathematics,* edited by M. Golubitsky and J. Guckenheimer (American Mathematical Society, Providence, 1986); (d) N. Gao and R. P. Behringer (unpublished); (e) G. Ahlers and I. Rehberg, Phys. Rev. Lett. **56**, 1373 (1986).

[3](a) D. T. J. Hurle and F. Jakeman, J. Fluid Mech. **47**, 667 (1971); (b) V. Steinberg, J. Appl. Math. Mech. **35**, 335 (1971); (c) D. Gutkowicz-Krusin, M. A. Collins, and J. Ross, Phys. Fluids **22**, 1443, 1457 (1979).

[4]E. Knobloch, A. Deane, J. Toomre, and D. R. Moore, in Proceedings of the American Mathematical Society Conference on Multiparameter Bifurcation Theory, edited by M. Golubitsky and J. Guckenheinmer, Arcata, 1985 (unpublished); E. Knobloch (unpublished).

[5]L. J. Tichacek, W. S. Kmak, and H. G. Drickamer, J. Phys. Chem. **60**, 660 (1956).

[6]V. Steinberg, G. Ahlers, and D. S. Cannell, Phys. Scr. **32**, 534 (1985).

[7]From our measurements we know that the relaxation time is usually of the order of 15–20 min. We waited at each point 90 min for small steps in ΔT (order of 4 mK). The vertical diffusion time that corresponds to mass diffusion is $\tau_D \sim d^2/D = 4500$ sec.

[8]The particular direction of propagation depends on slight asymmetries in the initial conditions. We were not able to observe any asymmetry in our apparatus on the level of our resolution in visualization ($\varepsilon = 10^{-3}$) of patterns which appear first in convection of pure water. However, the rounding near threshold in measurements of the Nusselt number was on the level of 0.1%.

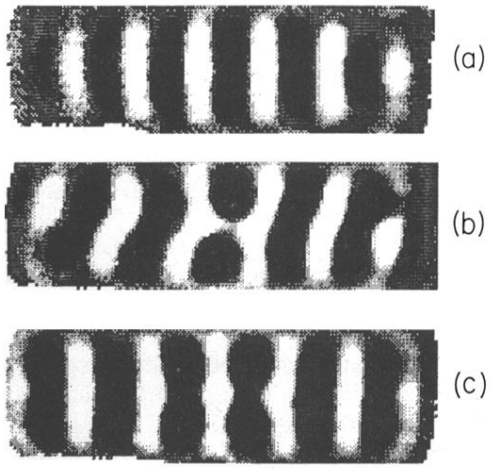

FIG. 2. Observed flow patterns in the cell with aspect ratio 1:4:12 for the sample 26 wt.% of ethanol at 28.185 °C. (a) Image of the flow patterns on the oscillatory convection branch; (b) image of "disordered" flow patterns on the oscillatory convection branch close to the point of the heteroclinic orbit; (c) image of the flow patterns on the stationary branch above the point of the heteroclinic orbit.